Influence of the Near-Wall Distance of a Single Cylinder on Flow-Induced Vibration and Heat Transfer Characteristics[#]

Yitong Fu [1,2], Dong Liu [1,2], Haoyu He [1,2], Tian Song [1,2], Lin Ding [1,2*]

1 Key Laboratory of Low-grade Energy Utilization Technologies and Systems of Ministry of Education of China, Chongqing University, Chongqing, China

2 School of Energy and Power Engineering, Chongqing University, Chongqing, China
(Corresponding Author: linding@cqu.edu.cn)

ABSTRACT

In this paper, the effect of near-wall distance on flow-induced vibration and heat transfer characteristics of a circular cylinder is numerically investigated. The amplitude ratio, frequency ratio, near-wake structure, and temperature distribution are analyzed. The results show that, the amplitude ratio increases with rising reduced velocity when $U^*{\leq}5$, and further increasing the reduced velocity leads to a transition of the cylinder's behavior from the upper branch to the lower branch. When $H{=}1D$, the cylinder obstructs the temperature boundary layer development, resulting in reduced heat transfer, accompanied by the highest average temperature (T_{mean}) and the lowest Nusselt number (Nu_{mean}); conversely, as the near-wall distance increases to $H{\geq}1.5D$, along with a rise in wall height, heat transfer enhances, yielding higher Nusselt numbers.

Keywords: Flow-induced vibration, vortex-induced vibration, convective heat transfer, near-wall distance, heat flux density

NONMENCLATURE

Abbreviations	
FIV	Flow-induced vibration
VIV	Vortex-induced vibration
Symbols	
A_y	Amplitude ratio
c	Damping of cylinder
D	Diameter of circular cylinder
f_n	Natural frequency of circular cylinder
k	Stiffness of cylinder
m^*	Mass ratio
q_w	heat flux density at wall
T	Temperature
T_∞	Incoming flow
U^*	Reduced velocity
U_∞	Incoming flow velocity

1. INTRODUCTION

In the contemporary era, high-performance computing devices, including central processing units (CPUs), graphical processing units (GPUs), and tensor processing units (TPUs), encounter thermal design challenges due to their significant heat generation and limited heat exchange surface area [1]. To optimize the performance of advanced computing systems, it is essential to incorporate efficient and compact cooling technology to maintain reliable and consistent operation. Air cooling is a popular choice due to its ease of installation and cost-efficiency. Two strategies can be employed to enhance forced convection heat transfer rates while maintaining specific temperature differentials [2-4]. One strategy involves expanding the surface area for heat dissipation. However, the dense packaging and compact design of advanced computers often limit the expansion of heat sink surface area. An alternative approach focuses on enhancing the heat transfer coefficient.

Enhancing the heat transfer coefficient through perturbations in the thermal boundary layer proves to be a highly effective method [5]. Nakamura and Igarashi [6] conducted wind tunnel experiments to explore transient heat convection around a circular cylinder within the Reynolds number range of 3000 to 15000. Within the sub-range of 5000 to 8000 Reynolds numbers, they observed the development of alternating flow reattachment at the cylinder's rear. This phenomenon led to a notable increase in both transient and time-averaged Nusselt numbers near the flow separation point.

Surface heat dissipation in computing equipment is commonly achieved through the use of constant heat flux walls. This heat dissipation can be significantly

---

[#] This is a paper for the 16th International Conference on Applied Energy (ICAE2024), Sep. 1-5, 2024, Niigata, Japan.

improved by increasing perturbations within the thermal boundary layer [7]. In light of this objective, the study examined the influence of a flexible cylinder positioned adjacent to a wall with a constant heat flux density, with the aim of enhancing heat transfer on the wall. The flow-induced vibration and heat transfer characteristics of the cylinder are discussed. The following sections are arranged as follows: in section 2, the physical model of a circular cylinder near heated wall is presented. In section 3, the method of numerical simulation is introduced. The results, include amplitude ratio, frequency ratio, near-wake structure, and temperature distribution are analyzed in section 4. In section 5, main conclusions are drawn.

2. PHYSICAL MODEL

Fig. 1 illustrates the physical model of a single-degree-of-freedom cylinder vibration in proximity to the wall. The circular cylinder of the vibration system is rigid body with a diameter denoted as D. The stiffness and damping of the vibration system are k and c respectively. The incoming flow is uniform, and the speed and temperature are U_∞ and T_∞ respectively. The flow medium is water, with density ρ and dynamic viscosity v. The mass ratio of the cylinder is $m^*=2$. The cylinder is situated in close proximity to a heated wall, with a near-wall distance H, and the wall experiences a heat flux density represented by q_w.
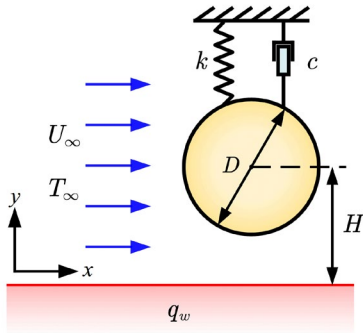
Fig. 1 Physical model

3. NUMERICAL APPROACH

In this study, the flow field parameters and the vibration response of the circular cylinder were obtained by solving the two-dimensional unsteady Navier-Stokes equation and the circular cylinder motion equation. The governing equations are as follows:

$$\frac{\partial u}{\partial x} + \frac{\partial v}{\partial y} = 0 \tag{1}$$

$$\frac{\partial u}{\partial t} + \frac{\partial uu}{\partial x} + \frac{\partial vu}{\partial y} = -\frac{\partial p}{\partial x} + \frac{1}{Re}\left(\frac{\partial^2 u}{\partial x^2} + \frac{\partial^2 v}{\partial y^2}\right) \tag{2}$$

$$\frac{\partial u}{\partial t} + \frac{\partial uu}{\partial x} + \frac{\partial vu}{\partial y} = -\frac{\partial p}{\partial x} + \frac{1}{Re}\left(\frac{\partial^2 u}{\partial x^2} + \frac{\partial^2 v}{\partial y^2}\right) \tag{3}$$

$$\frac{\partial \Theta}{\partial t} + \frac{\partial u\Theta}{\partial x} + \frac{\partial v\Theta}{\partial y} = \frac{1}{RePr}\left(\frac{\partial^2 u}{\partial x^2} + \frac{\partial^2 v}{\partial y^2}\right) \tag{4}$$

$$m\ddot{y} + c\dot{y} + ky = f_{y,fluid} \tag{5}$$

where x and y are dimensionless Cartesian coordinates, u and v are corresponding dimensionless velocity components in x, y direction. p is pressure. τ and ρ are dimension less time and density. Θ means dimensionless temperature, m is the mass of the circular cylinder, $f_{y,fluid}$ is the fluid force in y-direction acting on the cylinder.

Eq. (1-4) are solved by using ANSYS FLUENT which uses the finite volume method. The SST k-ω turbulence model is selected for simulation. The first order implicit scheme is used for temporal discretization, the convective term is discretized by second order upwind scheme, and the least squares cell-based method is used for calculating gradients. The motion equation Eq. (5) is solved by 4 order Runge-Kutta method. When the residual is less than 10^{-5}, it is determined that the calculation has converged. The computational domain is shown in Fig. 2. The size of the domain is $(L_1+L_2)\times H_1$, where $L_1=10D$, $L_2=20D$, and $H_1=20D$. The boundary conditions are as follows:

- Inlet: Uniform incoming flow;
- Outlet: pressure outlet;
- Top: free slip boundary;
- Cylinder surface: Adiabatic no-slip wall;
- Bottom: No-slip boundary with heat flux q_w;

The spatial discretization of calculation area employs a structured grid, and grid generation is performed using ICEM. The generated grid is presented in Fig. 3. This study uses an overset grid for calculation. The grid consists of a background grid and a component grid. The component grid is a circular area with a diameter of $2D$. The two sub-grids are generated independently and exchange data through the overset interface.

4. RESULTS

4.1 Vibration response

The amplitude ratio of the circular cylinder at different near-wall distances H with reduced velocity U^* are shown in Fig. 4. The reduced velocity is defined as $U^*=U_\infty/f_nD$, where f_n is the natural frequency of the circular cylinder. When $U^*\leq 5$, the amplitude ratio of the cylinder increases with the increasing reduced velocity, causing the vibration to transition from the initial branch to the upper branch. However, as the reduced velocity continues to rise, the amplitude ratio decreases with U^*

Top $\frac{\partial u}{\partial y} = 0, v = 0, \frac{\partial p}{\partial y} = 0, \frac{\partial T}{\partial y} = 0$

Inlet
$u = U_\infty$
$v = 0$
$T = T_\infty$

Outlet
$\frac{\partial u}{\partial x} = 0$
$\frac{\partial v}{\partial x} = 0$
$\frac{\partial T}{\partial x} = 0$

Bottom $q = q_w, \frac{\partial u}{\partial y} = 0, v = 0, \frac{\partial p}{\partial y} = 0$
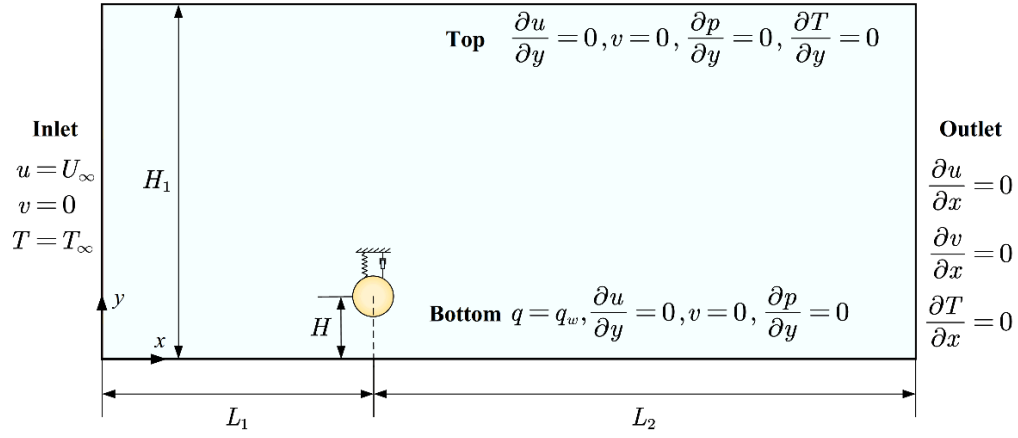
Fig. 2 Computational domain
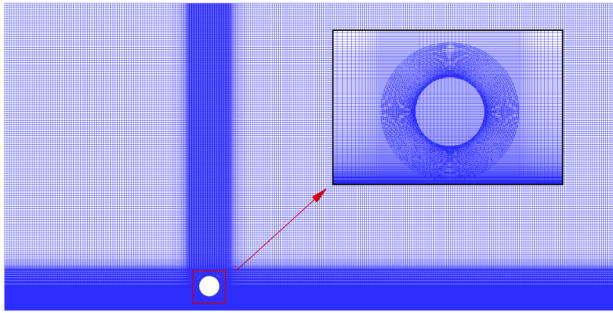
Fig. 3 Grid generation

increasing, until it reaches $U^* \geq 8$. In the U^* range of 9 to 14, except for the case with H=1D, the amplitude gradually increases with reduced velocity, leading to a transition of the vibration from the lower branch to the desynchronization region. Compared with FIV cases without considering wall heat flux [8], The reduced velocities with the maximum amplitude are all near U^*=5, and the maximum amplitude values are approximately equal. However, when wall heat flux is considered, the amplitude is higher at 8<U^*<14 than that in the case where wall heat flux is not considered.
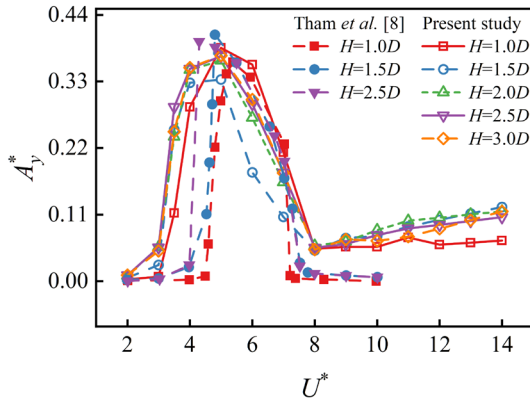
Fig. 4 Amplitude ratio at different near-wall distances

Fig. 5 presents the frequency ratio f/f_n of the circular cylinder at varying near-wall distances for different reduced velocities. For the case of H=1D, Frequency ratio demonstrates an increase with reduced velocity within the U^* range from 2 to 8. When the near-wall distance exceeds 1D, the frequency ratio displays vortex-induced vibration (VIV) response. Within the range of 2≤U^*≤4, the frequency ratio increases with the increasing reduced velocity. In the range of 5≤U^*≤7, the frequency response exhibits a locking phenomenon, and as a result, the corresponding vibration response becomes larger. When U^*≥8, The frequency ratio shows a linear increase as the reduced velocity rises.
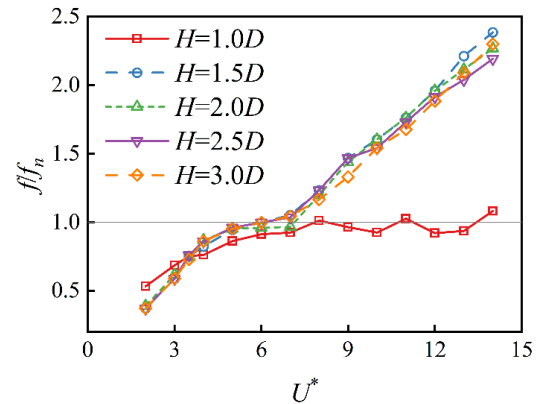
Fig. 5 Frequency ratio at different near-wall distances distances

4.2 Near-wake structures

The near wake structure of the cylinder under different near-wall distance at U^*=5 is presented in Figure 6. When H=1D and 1.5D (shown in Fig. 6(a) and (b)), the vorticity generated beneath the cylinder cancels out with the boundary layer on the wall, and only the shedding vortices in the wake region above the cylinder occur. A cylinder positioned too closely to the wall

impedes the development of the wall boundary layer. In cases where $H≥1.5D$, as the distance between the cylinder and the wall increases, vortices start to detach from the lower surface of the cylinder, resulting in the wake vortices adopting a 2S mode behavior. The vortices shed from the lower surface of the cylinder wrap around the boundary layer, inducing disturbances.
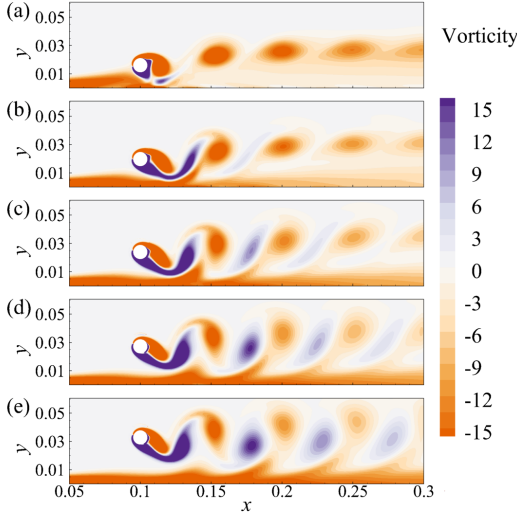
Fig. 6 Near wake structure under different near-wall distances at U^*=5 (a) H^*=1 (b) H^*=1.5 (c) H^*=2 (d) H^*=2.5 (e) H^*=3

Figure 7 illustrates the temperature distribution in the wake region of a circular cylinder at various near-wall distances at U^*=5. For the case of H=1D (shown in Fig.7 (a)), the cylinder obstructs the development of the temperature boundary layer in its wake, resulting in a diminished heat transfer effect. This condition leads to the highest average temperature T_{mean} and the lowest Nusselt number Nu_{mean} across all heights. As the near-wall distance increases, such as $H≥1.5D$, the wake created behind the cylinder disrupts the thermal boundary layer, thereby improving heat transfer. Furthermore, as the height near the wall increases, the heat transfer effect improves, resulting in larger Nusselt numbers.

5. CONCLUSIONS

In this study, the influence of near-wall distance on flow-induced vibration and convective heat transfer characteristics of a cylinder is investigated by numerical simulation. The results show that by arranging FIV cylinders on the constant heat flux wall, the temperature distribution near the wall can be effectively changed. This method can be used to enhance heat dissipation in actual engineering application scenarios such as chip heat dissipation. The amplitude ratio, frequency ratio,
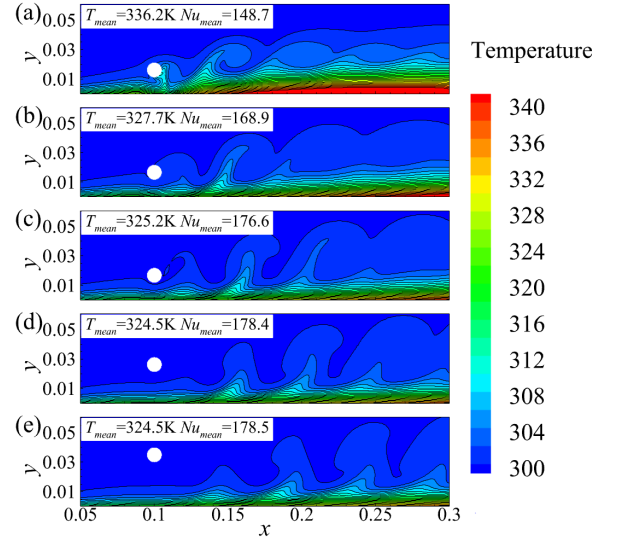
Fig. 7 Temperature distribution under different near-wall distances at U^*=5 (a) H^*=1 (b) H^*=1.5 (c) H^*=2 (d) H^*=2.5 (e) H^*=3

near-wake structure and temperature distribution are discussed. The main conclusions are drawn as follows:

a) When U^*≤5, the amplitude ratio increases with an increase in reduced velocity. As the reduced velocity continues to rise, the cylinder undergoes a transition from the upper branch to the lower branch, and the near-wall distance influences the amplitude response within the desynchronization region.

b) When H=1D or 1.5D, vortices shed only above the cylinder due to cancellation with the wall boundary layer, while closer proximity of the cylinder to the wall impedes boundary layer development; However, when $H≥1.5D$, increasing distance from the wall causes vortices to detach from the cylinder's lower surface, resulting in a 2S mode behavior and disturbance-inducing vortex wrapping around the boundary layer.

c) At H=1D, the cylinder hinders the development of the temperature boundary layer, resulting in decreased heat transfer, along with the highest average temperature (T_{mean}) and the lowest Nusselt number (Nu_{mean}); In contrast, with increased near-wall distance ($H≥1.5D$) and elevated wall height, heat transfer improves, leading to higher Nusselt numbers.

REFERENCE

[1] Go, J. S. Design of a microfin array heat sink using flow-induced vibration to enhance the heat transfer in the laminar flow regime. Sensors and Actuators a-Physical, 2003, 105(2): 201-210.

[2] Sun, X., Li, S., Lin, G. G., & Zhang, J. Z. Effects of flow-induced vibration on forced convection heat transfer from two tandem circular cylinders in laminar flow. International Journal of Mechanical Sciences, 2021, 195.

[3] Ding, L., Han, Y. X., Yang, Z. M., Zhang, L., & He, H. Y. Influence of upstream cylinder on flow-induced vibration and heat transfer of downstream cylinder. International Journal of Thermal Sciences, 2022, 176.

[4] Ali, U., Islam, M., Janajreh, I., Fatt, Y., & Alam, M. M. Flow-Induced Vibrations of Single and Multiple Heated Circular Cylinders: A Review. Energies, 2021, 14(24).

[5] Cheng, L., Luan, T., Du, W., & Xu, M. Heat transfer enhancement by flow-induced vibration in heat exchangers. International Journal of Heat and Mass Transfer, 2009, 52(3-4): 1053-1057.

[6] Nakamura, H., & Igarashi, T. Unsteady heat transfer from a circular cylinder for Reynolds numbers from 3000 to 15,000. International Journal of Heat and Fluid Flow, 2004, 25(5): 741-748.

[7] Yuan, L., Zou, S., Yang, Y., & Chen, S. Boundary-Layer Disruption and Heat-Transfer Enhancement in Convection Turbulence by Oscillating Deformations of Boundary. Physical Review Letters, 2023, 130(20): 204001.

[8] Tham, D. M. Y., Gurugubelli, P. S., Li, Z., & Jaiman, R. K. Freely vibrating circular cylinder in the vicinity of a stationary wall. Journal of Fluids and Structures, 2015, 59, 103-128.